Building Tomorrow's Society
Bâtir la Société de Demain

Fredericton, Canada
June 13 – June 16, 2018/ *Juin 13 – Juin 16, 2018*

SOIL-STRUCTURE INTERACTION MODELING OF FRP COMPOSITE PILES

Jafarian Abyaneh, Mostafa[1,4], El Naggar, Hany[1] and Sadeghian, Pedram[1]
[1] Department of Civil and Resource Engineering, Dalhousie University, 1360 Barrington Street, Halifax, NS, B3H 4R2 Canada
[4] mjafarianabyaneh@dal.ca

Abstract: Composite materials such as fibre-reinforced polymer (FRP) laminates have been widely used in civil engineering recently. The most important advantage of FRP composite piles compared to conventional concrete piles is the corrosion resistance which is an important factor in marine applications. In this research, an advanced numerical model has been proposed to address the mechanical behaviour of concrete-filled FRP tube (CFFT) pile. Furthermore, the interaction of composite pile with foundation soil was investigated under different lateral loadings. This model is based on nonlinear finite element analysis (NFEA) and disturbed state concept (DSC), which considers material and geometrical nonlinearity as well as the interface of soil with FRP layer and concrete. Moreover, the effect of relative stiffness of individual pile's components were studied on its structural and geotechnical performance utilizing 3D finite element models of full-scale field tests conducted during the construction of Route 40 Highway Bridge in Virginia. Based on the curves of deflection along the length of the pile, the modelling results were in good agreement with the experimental data. As a result, the proposed model can be used in a parametric study to optimize the design of composite piles. For the parametric study, different values for pile diameter-to-depth ratios and laminate thickness were investigated to address various governing parameters in the analysis and design of composite piles.

1 INTRODUCTION

Failure of a bridge component especially in the foundation due to corrosion can result in the collapse of the entire structure. Hence, durability and safety, as well as low maintenance of bridge structures, are of great concern to civil engineers and government bodies seeking for stable infrastructure. The replacement of corroded piles might be expensive and difficult because of superstructure relying on them (Roddenberry et al. 2014). In recent years, North American highway agencies and researchers have started to investigate the viability of protecting bridge piles with anti-corrosive materials such as fibre-reinforced polymer (FRP) composites, especially in the form of concrete-filled FRP tube (CFFT) piles (Fam et al. 2003).

In the literature, there are several research studies regarding FRP-wrapped concrete columns (FWCCs) (e.g., Ozbakkaloglu 2013, Cao et al. 2018, Silva and Rodrigues 2006, Mukherjee et al. 2004). They are different from CFFTs in several different aspects: First, FRP wraps are for existing structures and in these fibres are mainly oriented in the hoop direction. Whereas CFFTs are for new structures and various angles of fibres can be achieved. Second, in CFFTs concrete will after pouring into FRP tubes; while in FWCCs the concrete has already experienced most of shrinkage. Moreover, Biaxial stress is major effect in tubes, and FRP tubes contribute to axial capacity directly.

Fam and Rizkalla (2001) suggested an analytical model for predicting the behaviour of circular CFFTs by considering the bi-axial state of stress in FRP laminate. Mohamed and Masmoudi (2010a, 2010b) studied the axial and flexural behaviour of concrete-filled FRP and steel tubes experimentally and theoretically.

Ozbakkaloglu and Oehlers (2008) proposed a new method for making rectangular FRP tubes with unidirectional FRP sheets and investigated its effectiveness under axial compression tests. As the first pioneers in the FRP-wrapped concrete columns, CFFTs were initially proposed by Mirmiran and Shahawy (1996) acting as a mould for concrete similar to the ordinary concrete-filled steel tubes. Fam et al. (2005) investigated glass FRP concrete-filled rectangular filament-wound tube under axial and flexural loading with fibre oriented at ±45° and 90° with respect to the longitudinal axis. In the case of modelling, few numerical models were developed mainly for FRP-wrapped concrete columns such as the finite element analysis conducted by Yu et al. (2010) by using Drucker-Prager plasticity model.

Despite several investigations regarding CFFTs, few of the studies have elucidated the beneficial aspects of comprehensive numerical modelling for their mechanical behaviour. Furthermore, mechanical behavior of CFFTs was not previously considered in the soil-embedded composite piles as a load-bearing component under passive confinement. Moreover, most of them were analytical analysis conducted by researchers based on specific experimental results that cannot be applied to other experiments. As a result, the interface of FRP and soil needs to be considered in the models since the mechanism of concrete piles under the ground could be more complicated than conventional columns.

In this study, an advanced numerical model based on nonlinear finite element analysis (NFEA) was developed to predict the lateral deflection of CFFTs embedded in the soil. The failure criterion and damage model used in the modelling were based on Mohr-Coulomb plasticity model and disturbed state concept (DSC), respectively. For verification, experimental data from precast CFFT piles used in the construction of the new Route 40 Bridge in Virginia (Pando et al. 2006) has been used to obtain the model parameters under different loading conditions. The range of applied loads modelled in this research ranges from 11 kips to 27 kips. Furthermore, a parametric study was conducted by considering different values for the height-to-diameter ratio of specimens and angle of internal friction corresponding to the confining soil.

2 MODELLING

In CFFTs, there are two main structural components: an FRP shell or tube, and a concrete infill with or without steel reinforcement. The relative stiffness of these two components controls the pile's performance to vertical and lateral loads. By using nonlinear finite element analysis in three dimensions, a numerical model based on DSC damage model and Mohr-Coulomb failure criterion has been proposed to predict the complete elastic-plastic behaviour of CFFT piles under various lateral loading conditions. The values of applied lateral load modelled in this research are 11, 18, 21 and 27 kips. The interface of concrete, FRP and confining soil has also been investigated in the proposed model.

2.1 Disturbed state concept

The fundamental idea behind the applied model is based on disturbed state concept (DSC) damage model, which can be formulated as decomposition of material behaviour into its relatively intact (RI) and fully adjusted (FA) components. A schematic illustration of DSC has been shown in Figure 1. As can be seen in the figure, the blank and solid areas represent RI and FA parts, respectively. The initial response of the material is absolutely RI without any visible cracks. As applied displacement increases, the FA response becomes more predominant with the propagation of cracks resulting in entirely FA behaviour at the failure of the corresponding specimen. Based on the concept proposed by Desai (2001), the disturbance can be defined as:

$$[1]\quad D = D_u\left(1 - e^{-A\zeta_D^Z}\right)$$

where D_u is the ultimate value of disturbance; A and Z are material parameters; and ζ_D is the trajectory of deviatoric plastic strain as follows:

$$[2]\quad \zeta_D = \int \left(dE_{ij}^p dE_{ij}^p\right)^{\frac{1}{2}}$$

in which E_{ij} represents the deviatoric strain tensor of total strain tensor ε_{ij}. The disturbance of stress-strain curve can be generally expressed as:

$$[3]\ D = \frac{\sigma^{RI} - \sigma^{exp}}{\sigma^{RI} - \sigma^{FA}}$$

where σ^{exp}, σ^{RI}, σ^{FA}, are experimental, relatively intact (RI), fully adjusted (FA) stresses, respectively. The dependence of RI and FA states is different in the modelling procedure as a function of deviatoric plastic strain (Figure 1). As can be seen in the figure, the disturbance increases as the cracks propagate in the specimens. To find A and Z parameters, Equations [1] and [3] were equated for two arbitrary points of the experimental curve.

The disturbance parameters (Du, A, Z) were used for predicting the experimental behaviour of the corresponding material under independent tests. The dependence of RI and FA states is different in the modelling procedure. The modulus of elasticity and the type of adhesive material affect the RI behaviour, while the residual strength and confining conditions control the FA behaviour. After determination of disturbance parameters for each specimen, stress increments can be obtained by using following equation (Desai 2015):

$$[4]\ d\sigma_{ij} = (1-D)C^{ep}_{ijkl}d\varepsilon_{kl} + \frac{D}{3}\delta_{ij}C^{ep}_{ppkl}d\varepsilon_{kl} - dD(\sigma^{RI}_{ij} - \sigma^{FA}_{ij})$$

In the pre-failure stage where the value of D equals zero, Equation [4] stands for RI response. The RI state can be predicted by using different models from simple mathematical models to constitutive models such as the Mohr-Coulomb failure criterion. In this study, NFEA and Mohr-Coulomb plasticity model have been utilized in order to predict the RI response.

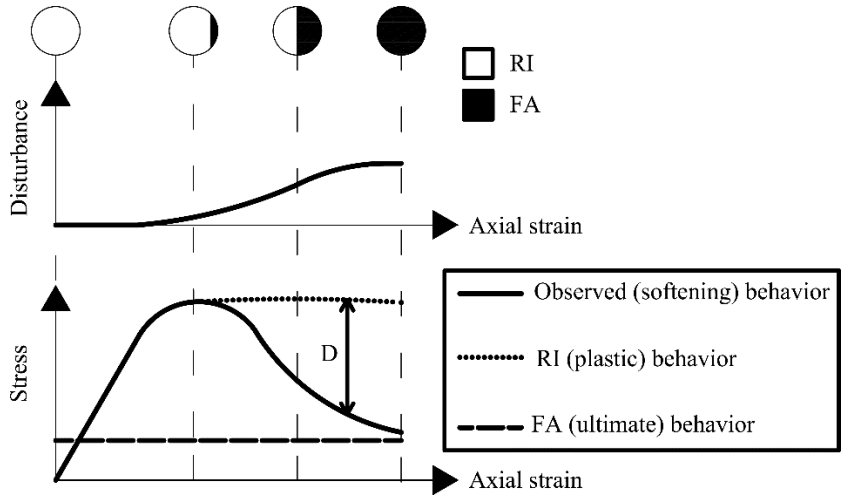

Figure 1: Schematic representation of DSC damage model based on the concept by Desai (2015)

2.2 Mohr-Coulomb Failure Criterion

The Mohr-Coulomb plasticity model allows to consider the effect of friction and interface problems. The corresponding yield surface plots as an irregular hexagon in the principal stresses space. One of the most important characteristics of this model is that it can provide different forms of strengths under various paths of stress or loading, for instance: simple shear, compression, and extension. Consequently, the aforementioned plasticity model is often considered to be more appropriate for frictional and geologic materials. The yield function of Mohr-Coulomb failure criterion can be shown as (Labuz and Zang 2012):

[5] $$F = J_1 \sin\phi + \sqrt{J_{2D}}\cos\theta - \frac{\sqrt{J_{2D}}}{3}\sin\phi\sin\theta - c\cos\phi$$

where J_1 and J_{2D} are the first invariant of stress and the second invariant of deviatoric stress, respectively. The parameters c and ϕ are cohesion and angle of friction of Mohr-Coulomb failure criterion. θ is the Lode angle which can be written as:

[6] $$\theta = \frac{1}{3}\sin^{-1}\left(-\frac{3\sqrt{3}}{2}\frac{J_{3D}}{J_{2D}^{3/2}}\right)$$

where J_{3D} is the third invariant of deviatoric stress. The value of θ must be acquired in the range of $[-\pi/6, \pi/6]$ (Toufigh et al. 2017).

3 PROPOSED MODEL

The model used in this research considers the following characteristics of CFFT and concrete piles as well as CFFT columns that are a special case of CFFT piles in three dimensions: (I) contact problem resulted from interface of concrete, FRP laminate and soil, (II) large deformation that was considered in several increments and iterations, (III) plasticity model by using hierarchical single surface (HISS) failure criterion, (IV) the softening effect of concrete in compression based on disturbed state concept (DSC).

As it can be seen in Figure 2, the initial steps in developing the model were defining the geometry of the problem, number of steps, elastoplastic parameters and Gaussian points for initial interpolation and final extrapolation of stress and strain values. By generating a finite element method (FEM) mesh, nodal freedom and loads can be determined.

A three-dimension mesh was generated for the cylindrical composite pile, and the horizontal cross-section of the cylinder has been shown in Figure 3. The inner radius of the cylinder (R_1) was assumed to be numerically zero. Each element was mapped to a cubic element with unit dimensions as shown for one arbitrary element in Figure 4. The stresses were calculated for eight quadratic Gaussian points in each element by using values of $3^{-1/2}$ for their coordinates with respect to unit value in each direction of the cube (Zienkiewicz and Taylor 2013). For extraction of modelling results, the stress values were extrapolated by the same reverse procedure for element nodes. As a result, cubic elements with unit dimensions were used for interpolation and extrapolation of stresses values instead of circular sector element.

For implementation of contact problem resulting from interface of composite pile and soil, separate mesh was generated for soil and contact elements. As can be seen in the figure, the interface of composite pile and soil was addressed by the blank elements between soil and concrete. Moreover, the friction and normal stress of soil with FRP and concrete were considered in the aforementioned interface elements.

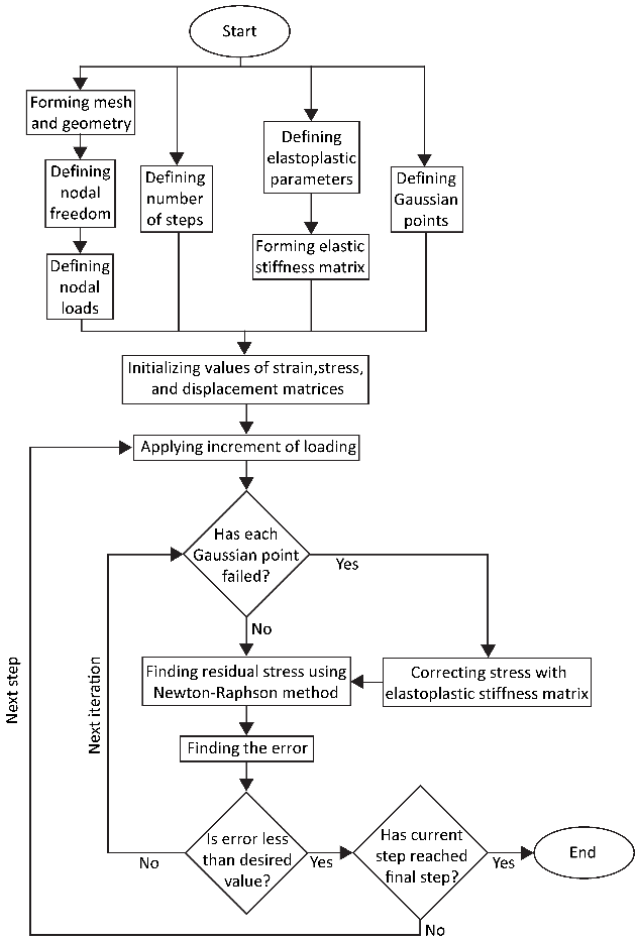

Figure 2: Flowchart of the proposed model for CFFT and normal concrete piles under lateral loading

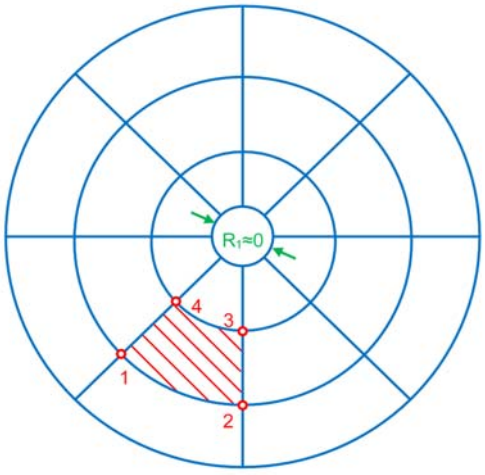

Figure 3: Schematic configuration of generated mesh in a horizontal direction

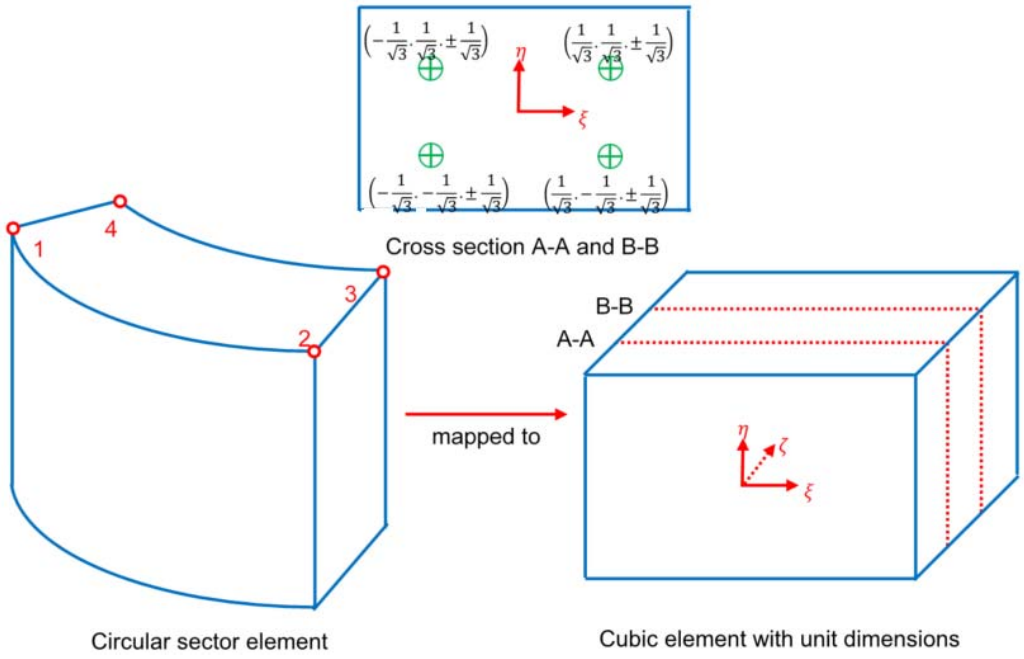

Figure 4: Mapping procedure used for quadratic interpolation and extrapolation of NFEA in three dimensions by considering eight Gaussian points.

Afterwards, the values of strain, stress, and displacement matrices were initialized. By applying the first increment of loading, the failure of each Gaussian point was checked. If the Gaussian point has failed, the elastic prediction should be corrected with elastoplastic stiffness matrix. To satisfy the equilibrium conditions between internal and external forces, the norm of following residual stress (**ψ**) must approach zero through required iterations (Khoei 2005):

$$[7]\quad \boldsymbol{\psi} = \int_V \bar{\mathbf{B}}\boldsymbol{\sigma} d_V - \mathbf{F}$$

where V is the volume of the specimen, **F** represents external forces tensor, **σ** is the Cauchy stress tensor and $\bar{\mathbf{B}}$ is the tensor relating the increments of strain and displacement ($\Delta\boldsymbol{\varepsilon} = \bar{\mathbf{B}}\Delta\bar{\mathbf{u}}$). In order to find the value of stress in each step of loading, the increment of stresses can be expressed as:

$$[8]\quad \begin{Bmatrix} \Delta\boldsymbol{\sigma}_r \\ \Delta\boldsymbol{\sigma}_\theta \\ \Delta\boldsymbol{\sigma}_z \\ \Delta\boldsymbol{\sigma}_{rz} \end{Bmatrix} = \mathbf{C} \begin{Bmatrix} \Delta\boldsymbol{\varepsilon}_r \\ \Delta\boldsymbol{\varepsilon}_\theta \\ \Delta\boldsymbol{\varepsilon}_z \\ \Delta\boldsymbol{\gamma}_{rz} \end{Bmatrix}$$

where **C** is the stiffness matrix, which can be elastic ($\mathbf{C}_e$) or elastic-plastic ($\mathbf{C}_{ep}$) depending on whether the corresponding Gaussian point has yielded or not. The indices *r*, *θ*, and *z* represent radial, angular, altitudinal components of stress and strain. Elastic-plastic stiffness matrix can be expressed as (Akhaveissy et al. 2009):

$$[9]\quad \mathbf{C}_{ep} = \mathbf{C}_e - \frac{\mathbf{C}_e \mathbf{n}\mathbf{n}^T \mathbf{C}_e}{H + \mathbf{n}^T \mathbf{C}_e \mathbf{n}}$$

where H is the hardening modulus, n is the flow rule vector that shows growth direction of the failure surface.

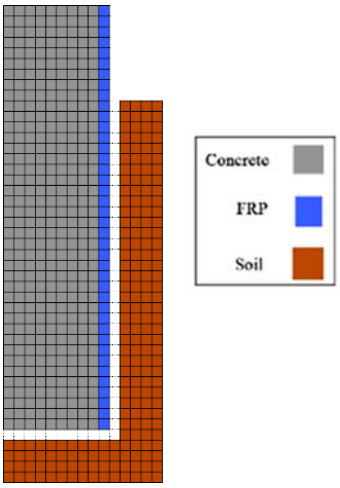

Figure 5: Schematic representation of generated mesh for the interface of concrete, FRP laminate and soil in the proposed model.

4 VERIFICATION

The experimental field test results from Fam et al. (2003) were used to verify the parameters of the proposed model. The composite piles were concrete-filled glass fibre reinforced polymer (GFRP) tubes considered for Route 40 Highway Bridge in Virginia with diameter and a wall thickness of 624.8 mm (24.6 in) and 5.33 mm (0.21 in), respectively. As can be seen in Figure 6, the profile of soil consisted of different types of soil including sand and clay with conditions of loose at the top and stiff at the bottom of soil layers. The cross-section of the concrete pile has also been depicted along the soil profile as well as an arbitrary cross section of A-A. The total length of composite pile is 13.1 m, including the length of the pile that was not covered in the soil.

The graph of modelling verification is shown in Figure 7 along the length of the pile for different values of lateral loads that were applied at the top of composite pile including 48.9 kN, 80.1 kN, 93.5 kN and 120.1 kN. As shown in the figure, it can be concluded that after the depth of seven meters, the lateral deflection of the composite pile is approximately zero. According to the experimental and numerical curves, modelling results were in good accordance with experimental data, which can be used to conduct a parametric study in the test above by using the results of the calibrated model. The mechanical properties of concrete, FRP and soil was depicted in Table 1.

Table 1. Mechanical parameters used in the proposed model.

	Parameter	Concrete	Soil	FRP
Elasticity	E* (MPa)	18681	16.12	15162
	ν	0.2	0.15	0.32
Plasticity	c (MPa)	1.196	0.1	-
	φ	55	22	-

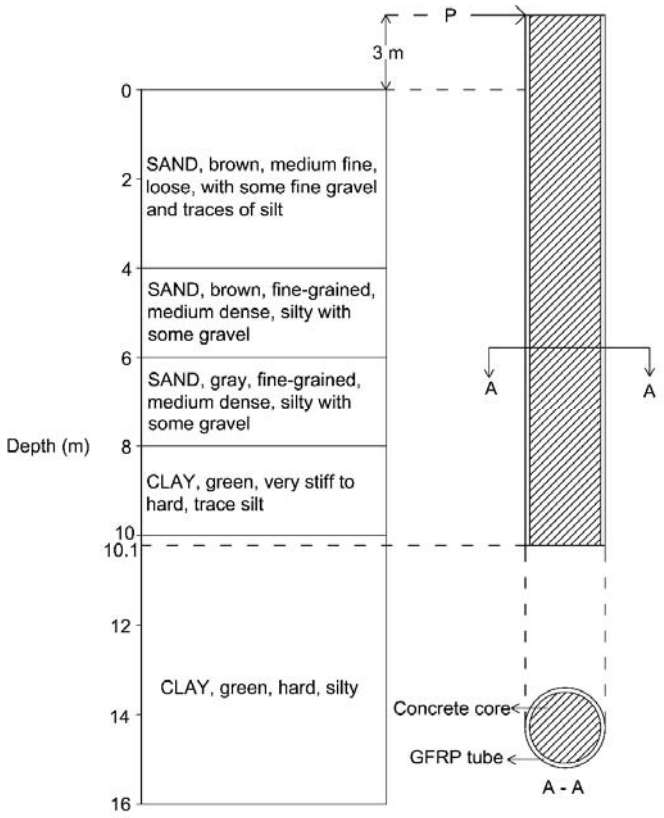

Figure 6: Soil and composite pile profiles along the depth (Fam et al. 2003)

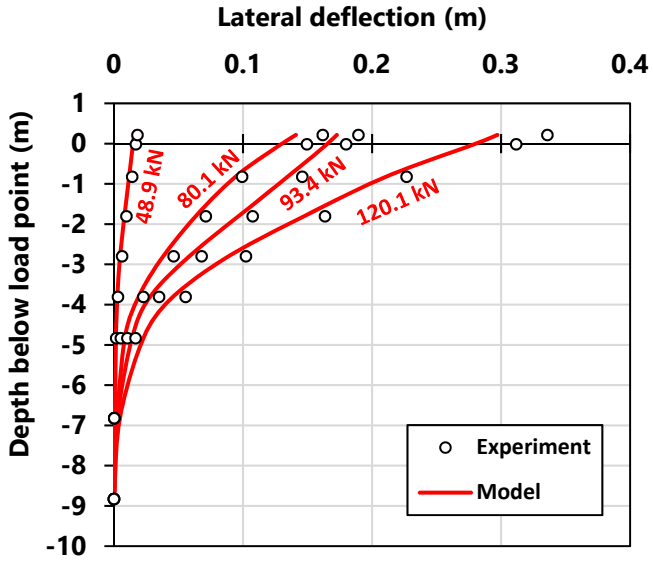

Figure 7: Verification of the model against field data of lateral deflection along the length of CFFT pile tested by Fam et al. (2003) at different lateral load levels ranging from 48.9 to 120.1 kN.

5 PARAMETRIC STUDY

Based on the generated model, the effect of different parameters such as length-to-diameter (L/D) ratio and FRP layer thickness (t) on the lateral deflection curve of concrete piles was studied along the depth under a certain amount of applied load.

1. Three different L/D ratios of 16, 22 and 28 were used in the proposed model to investigate the effect of the geometry on the lateral deformation of composite piles under a constant lateral load such as 48.9 kN as shown in Figure 8 (a). To find the variation of L/D along the length of composite pile, the value of length (L) was assumed to be 13.1 m as used previously. On the other hand, the diameter (D) was changed to allow for comparison of the results along the depth. As can be seen in the figure, the higher the L/D ratio in a certain depth, the more lateral deflection will be observed from the composite pile.

2. In order to find the effect of FRP thickness (t) on the mechanical behaviour of CFFT piles, the t values of 2, 5.33 and 8 mm were studied as depicted in Figure 8 (b). It can be seen that by having thicker FRP layer, the lateral deformation of CFFT pile will be reduced due to the higher strength of the composite material as well as providing better passive confining pressure for the CFFT piles. The failure of thicker layer occurred at a lower depth of 2.6 m, whereas the thinner layer started failing at a depth of 3.8 m.

6 CONCLUSION

In this study, an advanced constitutive model has been proposed to address the mechanical behaviour of concrete-filled FRP tube (CFFT) pile and its interaction with foundation soil under different lateral loadings. The proposed model is based on nonlinear finite element analysis (NFEA) and disturbed state concept (DSC), that considers material and geometrical nonlinearity as well as the interface of soil with FRP layer and concrete. Moreover, the effect of relative stiffness of individual pile's components was studied on its structural and geotechnical performance utilizing 3D finite element models of a full-scale field test conducted during the construction of Route 40 Highway Bridge in Virginia. Based on the curves of deflection along the length of the pile, the modelling results were in good accordance with the experimental data, which means that the proposed model can be used in a parametric study to optimize the design of composite piles. For the parametric study, different values for pile diameter-to-depth ratios and laminate thickness were investigated to address various governing parameters in the analysis and design of composite piles.

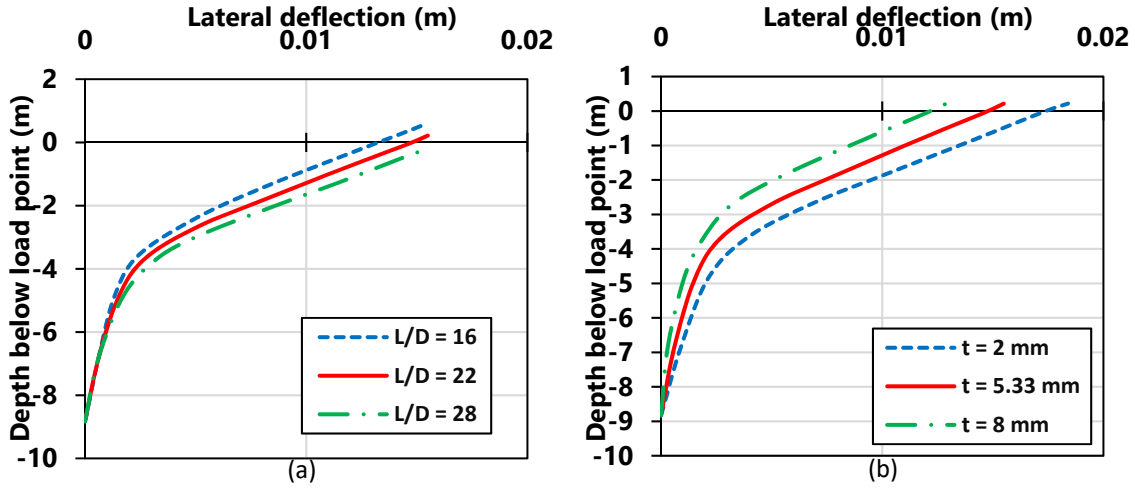

Figure 8: Parametric study of following parameters using the proposed model for the lateral deflection along the length of CFFT pile at lateral load of 48.9 kN: (a) slenderness ratio (b) FRP thickness.

References

Akhaveissy, A.H., Desai, C.S., Sadrnejad, S.A., and Shakib, H. 2009. Implementation and comparison of generalized plasticity and disturbed state concept for load-deformation behavior of foundation. *Scientia Iranica Transaction A Civil Engineering*, **16**(3), 189–198.

Cao, Y., Wu, Y.-F., and Jiang, C. 2018. Stress-strain relationship of FRP confined concrete columns under combined axial load and bending moment. *Composites Part B: Engineering*, **134**, 207-217.

Desai, C. S. 2001. *Mechanics of Materials and Interfaces: The Disturbed State Concept*. CRC Press.

Desai, C.S. 2015. Constitutive modeling of materials and contacts using the disturbed state concept: Part 1 – Background and analysis. *Computers & Structures*, **146**, 214–233.

Fam, A., and Rizkalla, S.H. 2001. Behavior of axially loaded concrete-filled circular FRP tubes. *Aci Structural Journal*, **98**(3), 280–289.

Fam, A., Pando, M., Filz, G., and Rizkalla, S. 2003. Precast piles for Route 40 bridge in Virginia using concrete filled FRP tubes. *PCI Journal*, **48**(3), 32–45.

Fam, A., Schnerch, D., and Rizkalla, S. 2005. Rectangular filament-wound glass fiber reinforced polymer tubes filled with concrete under flexural and axial loading: experimental investigation. *Journal of Composites for Construction*, **9**(1), 25–33.

Khoei, A.R. 2005. *Computational Plasticity in Powder Forming Processes*. Elsevier, Oxford, UK.

Labuz, J.F., and Zang, A. 2012. Mohr–Coulomb failure criterion. *Rock Mechanics and Rock Engineering*, **45**(6), 975-979.

Mirmiran, A. and Shahawy, M. 1996. A new concrete-filled hollow FRP composite column. *Composites Part B: Engineering*, **27**(3–4), 263–268.

Mohamed, H.M., and Masmoudi, R. 2010a. Axial load capacity of concrete-filled FRP tube columns: Experimental versus theoretical predictions. *Journal of Composites for Construction*, **14**(2), 231–243.

Mohamed, H.M., and Masmoudi, R. 2010b. Flexural strength and behavior of steel and FRP-reinforced concrete-filled FRP tube beams. *Engineering Structures*, **32**(11), 3789–3800.

Mukherjee, A., Boothby, T.E., Bakis, C.E., Joshi, M.V., and Maitra, S.R. 2004. Mechanical behavior of fiber-reinforced polymer-wrapped concrete columns—complicating effects. *Journal of Composites for Construction*, **8**(2), 97–103.

Ozbakkaloglu, T. 2013. Compressive behavior of concrete-filled FRP tube columns: Assessment of critical column parameters. *Engineering Structures*, **51**, 188–199.

Ozbakkaloglu, T., and Oehlers, D.J. 2008. Manufacture and testing of a novel FRP tube confinement system. *Engineering Structures*, **30**(9), 2448–2459.

Pando, M.A., Ealy, C.D., Filz, G.M., Lesko, J.J., and Hoppe, E.J. 2006. A laboratory and field study of composite piles for bridge substructures. Virginia Transportation Research Council 530 Edgemont Road Charlottesville, VA 22903.

Roddenberry, M., Mtenga, P., and Joshi, K. 2014. Investigation of Carbon Fiber Composite Cables (CFCC) in Prestressed Concrete Piles. *The Final report for Florida Department of Transportation*, Contract Number BDK83-977-17, FSU Project ID: 031045.

Silva, M.A., and Rodrigues, C.C. 2006. Size and relative stiffness effects on compressive failure of concrete columns wrapped with glass FRP. *Journal of Materials in Civil Engineering*, **18**(3), 334–342.

Toufigh, V., Jafarian Abyaneh, M., and Jafari, K. 2017. Study of Behavior of Concrete under Axial and Triaxial Compression. *ACI Materials Journal*, **114**(4), 619-629.

Yu, T., Teng, J.G., Wong, Y.L., and Dong, S.L. 2010. Finite element modeling of confined concrete-II: Plastic-damage model. *Engineering Structures*, **32**(3), 680–691.

Zienkiewicz, O.C., and Taylor, R.L. 2013. *The finite element method for solid and structural mechanics*. 7th ed., Butterworth-heinemann.